Integrated Bragg grating filter in ultra-thin silicon-on-insulator strip waveguides

Zhi Zou[a], Linjie Zhou*[a], Jianping Chen[a]
[a]State Key Laboratory of Advanced Optical Communication Systems and Networks, Department of Electronic Engineering, Shanghai Jiao Tong University, 800 Dongchuan Rd., Shanghai 200240, China

ABSTRACT

We demonstrate an integrated Bragg grating filter using 60-nm-thick silicon-on-insulator strip waveguides. The ultra-thin waveguides exhibit a propagation loss of 0.61 dB/cm. Upon thinning-down, the waveguide effective refractive index is reduced, making the fabrication of Bragg grating filter possible using the standard 248-nm deep ultra-violet (DUV) photolithography process. The Bragg grating filter exhibits a stopband width of 1 nm and an extinction ratio of 31 dB.

Keywords: Bragg grating, filter, silicon-on-insulator, waveguide

1. INTRODUCTION

Monolithically integrated Bragg gratings on the silicon-on-insulator (SOI) platform are highly desirable for next generation optical communications due to its compact size, narrow bandwidth selectivity, and compatibility with complementary metal oxide semiconductor (CMOS) technologies. In principle, the period of Bragg grating is inversely proportional to the effective refractive index of Bragg grating, which makes the fabrication of SOI Bragg gratings challenging due to the small grating period. Electron-beam lithography (EBL) is the workhouse for the fabrication of SOI Bragg gratings [1, 2], but it is time consuming and unsuitable for mass-production. In this work, we demonstrate an integrated Bragg grating filter based on the 60-nm-thick silicon strip waveguides fabricated by standard 248-nm DUV photolithography. To the best of our knowledge, this is the first time that a Bragg grating filter in ultra-thin silicon waveguides has been reported. With a reduced waveguide height, the propagating modes are less confined to the silicon cores and penetrate more into the surrounding silicon oxide, resulting in large evanescent fields and low effective refractive indices. This in turn enlarges the period of the Bragg grating filter and therefore makes it possible to fabricate using the 248 nm DUV photolithography. Moreover, ultra-thin silicon waveguides are less sensitive to waveguide sidewall roughness, a key factor that contributes to the waveguide propagation loss, and therefore, devices based on the ultra-thin waveguides could have a lower loss. Our experimental results show the waveguides with a height of 60 nm and a width of 900 nm have a propagation loss of only 0.61 dB/cm at 1.55 um, which is 5$\times$smaller than that of a regular 220-nm thick waveguide fabricated using the same process. The silicon Bragg grating filter exhibits a stopband width of 1 nm and an extinction ratio of 31 dB.

2. ULTRA-THIN WAVEGUIDE STRUCTURE AND FABRICATION

Figure 1(a) shows the cross section of the ultra-thin silicon waveguide. The waveguide height is 60 nm. A wider silicon core is necessary to guide the propagating mode. The single mode condition for waveguides with a 60-nm-thick silicon core is maintained with a waveguide width up to 1150 nm. The width of waveguide is designed to be 950 nm in our design. Simulation using Lumerical MODE Solutions shows that the waveguide has an effective index of n_{eff} = 1.69 at 1.55 μm, much lower than the effective index of 2.45 of a regular 500 nm (width) × 220 nm (height) silicon strip waveguide. Figure 1(b) illustrates the x-component of the electronic field distribution of the fundamental transverse electric (TE)-mode. The mode size, measured when field decays to 1/e of the maximum, is ~1 μm (width) × 0.6 μm (height). In contrast, the mode size for a regular waveguide is ~0.35 μm (width) × 0.25 μm (height).

AOPC 2015: Micro/Nano Optical Manufacturing Technologies; and Laser Processing and Rapid Prototyping Techniques, edited by Lin Li, Minghui Hong, Lan Jiang, Proc. of SPIE Vol. 9673, 96730J · © 2015 SPIE · CCC code: 0277-786X/15/$18 · doi: 10.1117/12.2199171

*s.greg.jones@narelab.com; phone 1 222 555-1234; fax 1 222 555-876; narelab.com

Downloaded From: http://proceedings.spiedigitallibrary.org/ on 10/20/2015 Terms of Use: http://spiedigitallibrary.org/ss/TermsOfUse.aspx

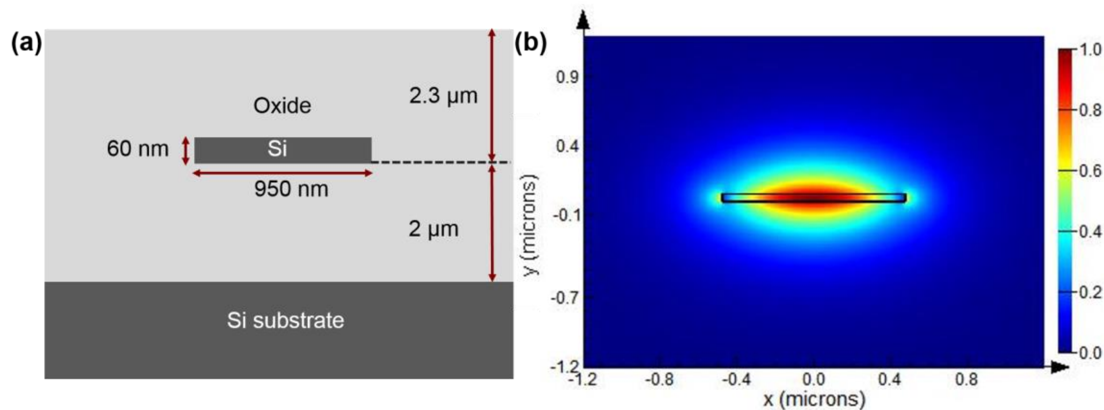

Figure 1. (a) Schematic of the ultra-thin waveguide cross section. (b) Simulated x-component of the electronic field distribution for the fundamental TE-mode.

The 60-nm-thick waveguide devices were fabricated together with other regular 220-nm-thick ridge waveguide devices. The fabrication was done using the IME standard CMOS fabrication process on a SOI wafer with a top silicon layer thickness of 220 nm and a buried oxide (BOX) layer thickness of 2 μm. The device patterns were defined by 248-nm DUV photolithography, followed by anisotropic dry etch of silicon. Three masks were used to pattern the silicon layer. The first mask defines the grating couplers with an etched depth of 70 nm for the 220-nm-thick devices. The second mask defines silicon waveguides with an etched depth of 160 nm. The third mask defines the remained slab region where the 60 nm silicon slab is etched down to the BOX layer. Hence, our ultra-thin waveguide devices were patterned by the third mask on the slab layer. A 2.3 μm thick silicon dioxide layer was deposited using plasma-enhanced chemical vapor deposition (PECVD) as the device upper-cladding.

3. EXPERIMENTAL RESULTS

We used the Agilent loss and dispersion analyzer (86038B) to characterize the device transmission performance. A polarization controller was placed in front of the device to set the TE polarization. A pair of on-chip grating couplers couple light into and out of the device from optical fibers. Figure 2(a) shows the scanning electron microscope (SEM) image of the grating coupler. The waveguide is adiabatically tapered to expand the waveguide mode. The grating period is fixed at 1.08 μm, while the trench width linearly increases from 0.34 μm (near the waveguide end) to 0.54 μm with a step of 40 nm in order to generate a longitudinal Gaussian profile of the diffracted field. Figure 2(b) shows the measured output spectrum after light passes through a pair of grating couplers connected by a 1 cm long waveguide. The fiber-to-fiber insertion loss is around 13 dB at the central wavelength of 1565 nm and the 1 dB bandwidth is around 40 nm. To evaluate the propagation loss of the ultra-thin silicon waveguides, we measured the insertion losses of a series of waveguides with an incremental length. Figure 2(c) shows the experimental data from three chips fit by a straight line. The average propagation loss of the waveguides is 0.61 ± 0.08 dB/cm deduced from the linear fitting. This waveguide loss is $5\times$ smaller than that of a regular 500 nm $\times$ 220 nm waveguide using the same fabrication process as reported in our previous work [3]. The low overlap and interaction between the waveguide mode and the sidewall roughness in the ultra-thin waveguides greatly reduce the scattering loss, leading to the much lower waveguide propagation loss.

Downloaded From: http://proceedings.spiedigitallibrary.org/ on 10/20/2015 Terms of Use: http://spiedigitallibrary.org/ss/TermsOfUse.aspx

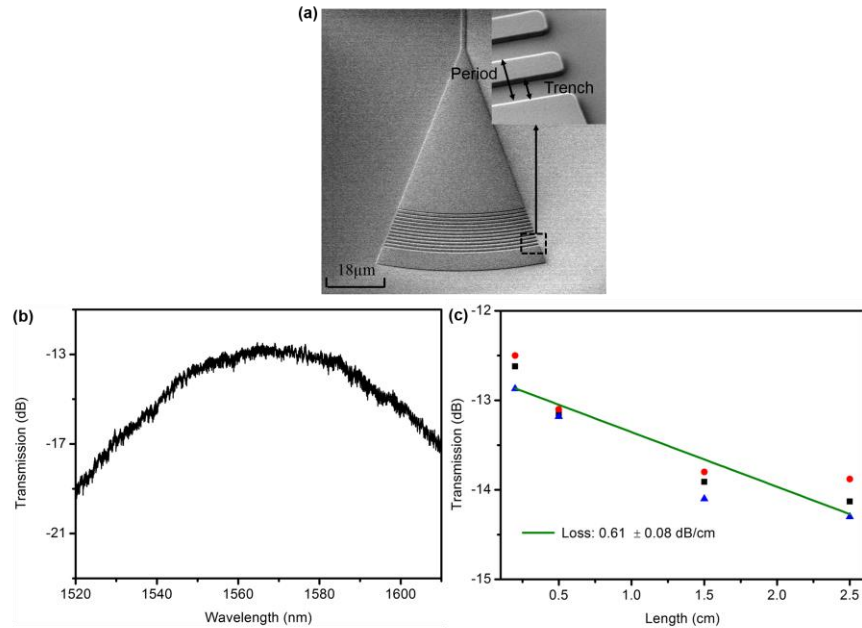

Figure 2. (a) SEM image of the grating coupler. (b) Transmission spectrum of a test waveguide with a pair of grating couplers. (c) Waveguide propagation loss characterization. Each marker denotes a measured loss for a certain waveguide length. The solid line is linear fitting to the experimental data.

Figure 3(a) shows the schematic of the Bragg grating filter with an inward grating profile apodized by a tanh function. The Bragg grating filter has a width W of 900 nm, a grating length L of 5 mm, a side corrugation depth w of 70 nm and a grating period Λ of 473.4 nm. The full width at half maximum (FWHM) of the employed tanh apodization function of order 12 is 3.9 μm. Figure 3(b) shows the SEM image of a part of the Bragg grating filter. The solid line in Fig. 3(c) shows the measured transmission intensity spectrum. The width of the stopband is ~1 nm and the extinction ratio is 31 dB. The dotted line is the simulation spectrum with W and w as fitting parameters based on the GratingMOD module from the RSOFT. From fitting, we get W = 890 nm and w = 30 nm. The grating width is close to the designed value. However, the corrugation depth is much smaller than the designed value. The discrepancy may originate from the approximate effect incurred in photolithography [4]. The SEM photo in Fig. 3(b) confirms the grating teeth is significantly smoothed after fabrication. The discrepancy between the experimental and simulation results may be due to waveguide dimension variations that perturb the mode effective index [5, 6].

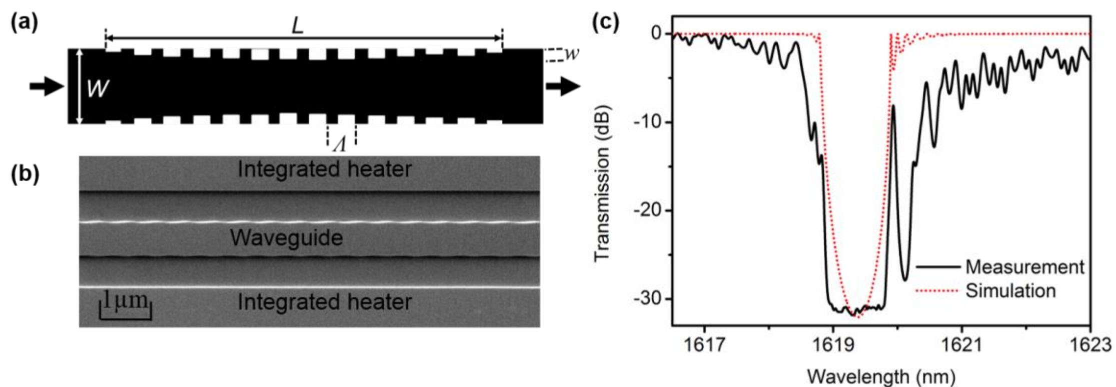

Figure 3. (a) Schematic structure of the Bragg grating filter. (b) SEM image of the Bragg grating filter. (c) Measured and simulated transmission spectra.

Downloaded From: http://proceedings.spiedigitallibrary.org/ on 10/20/2015 Terms of Use: http://spiedigitallibrary.org/ss/TermsOfUse.aspx

4. CONCLUSIONS

In conclusion, we have demonstrated an integrated Bragg grating filter in 60-nm-thick strip waveguides on the SOI platform. The ultra-thin waveguide exhibits a propagation loss of 0.61 dB/cm. By reducing the waveguide height, the effective index of the waveguide reduces and in turn enlarges the grating period, making it possible to realize Bragg gratings using the 248-nm DUV photolithography. The fabricated Bragg grating filter has been demonstrated to possess a stopband width of 1 nm and an ER of 31 dB.

5. ACKNOWLEDGMENTS

This work was supported in part by the 973 program (2011CB301700), the 863 program (2013AA014402), the National Natural Science Foundation of China (NSFC) (61422508), Science and Technology Commission of Shanghai Municipality (STCSM) Project (14QA1402600). We also acknowledge L. Jia of IME Singapore for device fabrication.

REFERENCES

[1] X. Wang, Y. Wang, J. Flueckiger, R. Bojko, A. Liu, A. Reid, J. Pond, N. A. F. Jaeger, and L. Chrostowski, "Precise control of the coupling coefficient through destructive interference in silicon waveguide Bragg gratings," Opt. Lett., vol. 39, 5519-5522 (2014).

[2] A. D. Simard, M. J. Strain, L. Meriggi, M. Sorel, and S. LaRochelle, "Bandpass integrated Bragg gratings in silicon-on-insulator with well-controlled amplitude and phase responses," Opt. Lett., vol. 40, 736-740 (2015).

[3] Z. Zou, L. Zhou, X. Sun, J. Xie, H. Zhu, L. Lu, X. Li, J. Chen, "Tunable two-stage self-coupled optical waveguide resonators," Opt. Lett., vol. 38, 1215–1217 (2013).

[4] Q. Fang, X. Tu, J. Song, L. Jia, X. Luo, Y. Yang, M. Yu, and G. Lo, "PN-type carrier-induced filter with modulatable extinction ratio," Opt. Express, vol. 22, 29914-29920 (2014).

[5] A. D. Simard, G. Beaudin, V. Aimez, Y. Painchaud, and S. LaRochelle, "Characterization and reduction of spectral distortions in Silicon-on-Insulator integrated Bragg gratings," Opt. Express, vol. 21, 23145-23159 (2013).

[6] A. D. Simard, N. Ayotte, Y. Painchaud, S. Bedard, and S. LaRochelle, "Impact of sidewall roughness on integrated Bragg gratings," J. Lightw.Technol., vol. 29, 3693-3704 (2011).

Downloaded From: http://proceedings.spiedigitallibrary.org/ on 10/20/2015 Terms of Use: http://spiedigitallibrary.org/ss/TermsOfUse.aspx